Cytomegalovirus MicroRNA Expression Is Tissue Specific and Is Associated with Persistence

JOURNAL OF VIROLOGY, Jan. 2011, p. 378–389 Vol. 85, No. 1
0022-538X/11/$12.00 doi:10.1128/JVI.01900-10

Cytomegalovirus MicroRNA Expression Is Tissue Specific and Is Associated with Persistence▽

Christine Meyer,[1] Finn Grey,[2] Craig N. Kreklywich,[1,3,4] Takeshi F. Andoh,[1,3,4] Rebecca S. Tirabassi,[5] Susan L. Orloff,[1,3,4] and Daniel N. Streblow[1,4]*

Department of Molecular Microbiology and Immunology and The Vaccine and Gene Therapy Institute, Oregon Health and Science University, Portland Oregon 97239[1]; Department of Surgery, Oregon Health and Science University, Portland Oregon 97239[3]; Portland VA Medical Center, Portland, Oregon 97239[4]; Roslin Institute and Royal School of Veterinary Studies, University of Edinburgh, Edinburgh, Scotland[2]; and University of Wisconsin—Madison, Madison, Wisconsin[5]

Received 8 September 2010/Accepted 19 October 2010

MicroRNAs (miRNAs) are a class of small noncoding RNAs involved in posttranscriptional regulation. miRNAs are utilized in organisms ranging from plants to higher mammals, and data have shown that DNA viruses also use this method for host and viral gene regulation. Here, we report the sequencing of the small RNAs in rat cytomegalovirus (RCMV)-infected fibroblasts and persistently infected salivary glands. We identified 24 unique miRNAs that mapped to hairpin structures found within the viral genome. While most miRNAs were detected in both samples, four were detected exclusively in the infected fibroblasts and two were specific for the infected salivary glands. The RCMV miRNAs are distributed across the viral genome on both the positive and negative strands, with clusters of miRNAs at a number of locations, including near viral genes *r1* and *r111*. The RCMV miRNAs have a genomic positional orientation similar to that of the miRNAs described for mouse cytomegalovirus, but they do not share any substantial sequence conservation. Similar to other reported miRNAs, the RCMV miRNAs had considerable variation at their 3′ and 5′ ends. Interestingly, we found a number of specific examples of differential isoform usage between the fibroblast and salivary gland samples. We determined by real-time PCR that expression of the RCMV miRNA miR-r111.1-2 is highly expressed in the salivary glands and that miR-R87-1 is expressed in most tissues during the acute infection phase. Our study identified the miRNAs expressed by RCMV *in vitro* and *in vivo* and demonstrated that expression is tissue specific and associated with a stage of viral infection.

MicroRNAs (miRNAs) are small noncoding RNAs involved in posttranscriptional regulation through binding to complementary sequences in target mRNAs resulting in gene silencing (4). miRNAs are ubiquitous among multicellular eukaryotic organisms, including plants and higher mammals, and have diverse roles in many different biological processes, including development, differentiation, proliferation, apoptosis, and hematopoiesis (35, 51). In addition to eukaryotic miRNAs, DNA viruses, mainly of the *Herpesvirus* family, have been shown to encode miRNAs. Bioinformatic, sequencing, and direct cloning approaches have led to the identification of more than 140 viral miRNAs (reviewed in reference 55). The role of viral miRNAs is proposed to include the targeting of cellular genes to induce a favorable replication environment or to evade the host immune system and the targeting of their own viral genome to regulate viral gene expression during persistence or latency/reactivation (22, 55).

Human cytomegalovirus (HCMV) is known to encode at least 14 miRNAs. HCMV is a ubiquitous betaherpesvirus, and primary infection results in lifelong persistent/latent infection of the host. Infection of immunocompetent hosts is generally asymptomatic, but infection of immunocompromised hosts can lead to high morbidity and mortality. HCMV has been linked to the development of atherosclerosis, arterial restenosis following angioplasty, and solid-organ transplant vascular sclerosis (TVS) (40, 41, 57). HCMV infection nearly doubles the 5-year rate of cardiac graft failure due to accelerated TVS (20) and doubles the rate of liver graft loss at 3 years (14, 52). Since the betaherpesviruses, including HCMV, are highly species specific, effective animal models have been established to investigate the role of CMV infection in chronic disease. We have utilized a rat cytomegalovirus (RCMV) infection system to model a number of human diseases associated with HCMV infections, including solid-organ transplant rejection and restenosis following angioplasty (26, 27, 29–31, 36–39, 45, 46, 56, 58, 62–64). Similar to human infection, infection of immunocompetent rats leads to a limited subclinical infection that persists lifelong in host bone marrow and columnar epithelial cells of the salivary glands (28). RCMV infection of immunocompromised rats (i.e., rats undergoing immunosuppressive treatment for the prevention of allograft rejection) leads to infection of most host tissues and organs. We have shown that RCMV gene expression is highly restricted in tissues from allograft recipients following infection. In fact, the highly expressed genes in tissues from the infected rats are hypothesized to be involved in host cell manipulation and/or immune evasion, which allows the virus to persist by turning over small amounts of infectious virus while remaining undetected by the immune system (65). However, the mechanisms by which CMV controls viral gene expression *in vivo* are still unknown. Recent studies suggest

* Corresponding author. Mailing address: Vaccine and Gene Therapy Institute, Oregon Health and Science University, 505 SW 185th Avenue, Beaverton, OR 97006. Phone: (503) 418-2772. Fax: (503) 418-2719. E-mail: streblow@ohsu.edu.

▽ Published ahead of print on 27 October 2010.

TABLE 1. Distribution of small RNAs in RCMV-infected fibroblasts and salivary glands

Cells	Sequence no.	Sequence %	Family no.	Family %
RCMV-infected fibroblasts				
Raw	6,665,287	100.00	414,447	100.00
Mappable	3,731,474	55.98	27,168	6.56
Mapped (total)	2,754,863	41.33	13,288	3.21
Unmapped (total)	976,611	14.65	13,880	3.35
Mapped to RCMV genome	305,522	4.60	1,611	0.39
RCMV-infected salivary glands				
Raw	7,230,718	100.00	377,359	100.00
Mappable	2,909,115	40.23	20,029	5.31
Mapped (total)	2,369,736	32.77	11,139	2.95
Unmapped (total)	539,379	7.46	8,890	2.36
Mapped to RCMV genome	4,159	0.06	145	0.03

that miRNAs may play an important role in regulating CMV gene expression and latency (23). The aim of the present study was to identify the miRNAs encoded in the RCMV genome and determine expression levels in tissue culture-infected fibroblasts, as well as in persistently infected tissues from RCMV-infected heart allograft recipients. Our elucidation of the RCMV miRNAs expressed during lytic and persistent *in vivo* infections is crucial for our understanding of their role in CMV persistence, pathogenesis, and disease.

MATERIALS AND METHODS

RCMV. The titers of salivary gland-derived stocks of the Maastricht strain of RCMV were determined using primary rat lung fibroblasts (RFL6 cells) (5, 6). Plaque assays were performed in confluent 24-well plates by infection with an appropriate serial virus dilution in 0.2 ml of medium and then incubation at 37°C for 90 min. Following incubation, the infected cells were rinsed with phosphate-buffered saline (PBS) and overlaid with 1 ml Dulbecco's modified Eagle's medium (DMEM) supplemented with 10% fetal calf serum (FCS), nonessential amino acids, penicillin-streptomycin, and 20 mM L-glutamine with a final concentration of 0.6% agarose. After 7 days, the cells were fixed in 3.7% formaldehyde in PBS and stained with 0.05% aqueous methylene blue. The plaques were counted by light microscopy.

RCMV infection of tissue culture cells. RFL6 cells were maintained in DMEM supplemented with 10% FCS and penicillin-streptomycin-glutamine (42, 62). For the cloning and sequencing of the RCMV miRNAs from *in vitro*-infected cells, RFL6 cells were plated onto 150-mm dishes (Costar). These cells were infected with RCMV upon confluence at a multiplicity of infection (MOI) of 0.1. After 3 h, the cells were washed three times with PBS. The infected cells were harvested at 72 h postinfection (hpi) by one washing with PBS and then addition of 3 ml of Trizol reagent. The reagent was allowed to lyse the cells for 5 min at room temperature. Subsequently, the samples were stored frozen at −80°C. For miRNA real-time PCR analysis of the RCMV miRNAs miR-R87-1 and miR-r111.2-6 in infected tissue culture cells, RFLs were plated into six-well plates. The cells were infected with RCMV (MOI of 0.1) and harvested by addition of Trizol, as described above, at 6, 24, and 48 hpi.

Preparation of rat tissues from heart allograft recipients. To identify the RCMV miRNAs expressed *in vivo*, we sequenced the small RNAs from total RNA samples isolated from salivary glands from rat allograft recipients at 21 days postinfection (dpi) (62, 65). Rat heart transplant surgeries were performed as previously described (45, 62–65). Various tissues (native and graft heart, salivary gland, spleen, liver, kidney, and lung) were collected from infected heart allograft recipients at 7 and 28 dpi (61, 62, 65) for real-time PCR analysis of the RCMV miRNAs miR-R87-1 and miR-r111.1-2. For each analysis, total RNA was prepared from approximately 0.25 g of rat tissue using the Trizol method. All animals were housed in the Portland VA Medical Center animal facilities in a specific-pathogen-free room. This facility is AAALAC accredited and complies with the requirements for animal care stipulated by the USDA and HHS.

miRNA deep sequencing. Deep sequencing was performed by LC Sciences (Houston, TX). Accordingly, for each sample, about 10 μg of total RNA was size fractionated on a 15% Tris-borate-EDTA (TBE) urea polyacrylamide gel and a 15- to 50-bp fraction was excised. The small RNA fraction was eluted from the gel slice in 500 μl of 0.3 M NaCl and precipitated by the addition of ethanol. According to the Illumina Solexa instructions, both 5′ and 3′ RNA adaptors were added using T4 RNA ligase and the ligated RNA was again size fractionated on a 15% TBE polyacrylamide gel. The fraction containing the 65- to 100-bp region was excised from the gel and precipitated. The recovered RNA was converted to single-stranded cDNA using Moloney murine leukemia virus reverse transcriptase (RT) and the Illumina Solexa RT primer. The cDNA was amplified with *Pfx* DNA polymerase for 20 cycles by PCR using the Illumina Solexa small RNA primer set. PCR products were purified on a 12% polyacrylamide gel, and the 80- to 120-bp fraction was excised from the gel and eluted and precipitated as described above. The samples were resuspended and sequenced using the Illumina Solexa G1 sequencer. Raw sequencing data were filtered for composition, the presence of adaptor dimers, length, sequence repetition, and copy number. The filtered data were then mapped to current miR databases, the *Rattus norvegicus* genome, and the RCMV genome (AF232689).

Northern blot analysis. Total RNA was isolated from infected (72 hpi) or uninfected rat fibroblasts using the Trizol (Invitrogen) method. To determine the kinetics of RCMV miRNA gene expression, another set of fibroblasts were harvested at 0, 8, 48, and 48 hpi in the presence of foscarnet (1:250 125 mM). Equal volumes of formamide and loading dye were added to each 20-μg sample of RNA. The samples were boiled for 5 min and cooled on ice prior to loading onto a 15% urea-acrylamide gel. The gel was transferred to GeneScreen plus (Perkin-Elmer) membrane in 1× TBE. Probes were produced by end labeling oligonucleotides using polynucleotide kinase (Fermentas) with [γ-^{32}P]dATP. The total labeled probe was hybridized to the blot overnight at 38°C in PerfectHyb Plus (Sigma Aldrich). The blot was washed two times with a low-stringency buffer (2× SSC [1× SSC is 0.15 M NaCl plus 0.015 M sodium citrate], 0.05% sodium dodecyl sulfate [SDS]) and one time with a high-stringency buffer (0.1× SSC, 0.1% SDS) at 38°C. The blot was exposed to autoradiographic film (Kodak BioMax MS) overnight at −80 C.

Quantitative RT-PCR detection of RCMV miRNAs. Real-time RT-PCR was used to quantify the RCMV miRNA expression in RCMV-infected fibroblasts and tissues from RCMV-infected heart allograft recipients. miRNA cDNA was generated from total RNA using the TaqMan microRNA reverse transcription kit (Applied Biosystems) in 15-μl reaction mixtures containing 1.5 pmol of the miRNA-specific RT primer and 100 ng of total RNA. The sequences of the miR-R87.1 and miR-r111.1-2 RT primers are GTC GTC TCC AGT GCA GGG TCC GAG GTA TTC GCA CTG GAT ACG ACG AGTT G and GTC GTC TCC AGT GCA GGG TCC GAG GTA TTC GCA CTG GAT ACG ACA CGC CG, respectively. Samples were incubated in an Applied Biosystems 9700 thermocycler at 16°C for 30 min, 42°C for 30 min, and then 85°C for 5 min. Real-time PCR (TaqMan) was used to quantify miRNA levels from 1.5 μl of the cDNA reaction mixture run in a ABI StepOnePlus real-time PCR machine using 40 cycles of 95°C for 15 s and 60°C for 1 min (63–65). The primer and probe sets used included miR-R87-1 forward primer GCT CGA AGA ACG GGT GC, reverse primer GTG CAG GGT CCG AGG T, and probe TGG ATA CGA CGA GTT G and miR-r111.1-2 forward primer GCT CGA AAC AAC GTG GA, reverse primer GTG CAG GGT CCG AGG T, and probe TGG ATA CGA CAC GCC G. Oligonucleotides with the miRNA sequences for miR-R87-1 and miR-r111.1-2 were used as quantification standards. Data are presented as relative copy numbers per 10 ng of total input RNA.

TABLE 2. RCMV miRs detected in infected fibroblasts and salivary glands

RCMV-miR name	miR sequence[b]	miR length (nt)	Copy no. of isoform	Copy no. of all isoforms	Strand	Genomic position[a]	
						miR start	miR end
Sequenced from RCMV-infected fibroblasts (72 hpi)							
miR-r6-1	TCGACCTCAAGCCGTTCGGGAC	22	131	996	+	8671	8692
miR-OriLyt-1	GACGGGGTCTCGGGCTCCTGA	21	178	583	+	77402	77422
miR-OriLyt-2	TGGCTCGCGTCGCCATGGAGAC	22	30	97	+	78953	78974
miR-R87-1	TCGAAGAACGGGTGCAACTC	20	68,629	166,117	+	113930	113949
miR-R91-1	GGACTCGGAGTCGTCGGACGCT	22	1,706	6,491	+	121165	121186
miR-r111.1-1	CGCACCGGCGTCGAGCACGTAC	22	753	2,857	+	152214	152235
miR-r111.1-2	TCGAAACAACGTGGAACGGCGT	22	11,212	30,084	+	152728	152749
miR-r111.1-3	TCGGGGGCGGTCGGAAGGTCC	21	78	427	+	152891	152911
miR-r1-1	GTAAGATGGAATCACCGGAGG	21	5,265	26,402	−	1024	1044
miR-r1-2	TTTCTCTCGTGCTCCGTGTCGC	22	610	1,030	−	1187	1208
miR-r1-3	TGATGCGGGGTAGGGGAGTGAG	22	183	473	−	1154	1175
miR-r1-4	CCAGGTGGAGGAGTCCGGTC	20	85	156	−	1281	1300
miR-r37-1	TTGTCGTGGGTTTCGT	16	72	77	−	34740	34755
miR-r43.1-1	TTATCAGCCGGCAAGCACCCAGG	23	1,261	5,577	−	40748	40770
miR-r43.1-2	AGGGGTTCGCCGGCCGATATCG	22	40	58	−	40795	40816
miR-R90-1	GACCGGGGATCGTCGAACGAC	21	66	192	−	121129	121149
miR-r111.2-1	TACGTGCTCGACGCCGGTGCGG	22	13	47	−	152213	152234
miR-r111.2-2	CTTCGAGTGCGTGTCCGATAGC	22	101	347	−	152238	152259
miR-r111.2-3	AATCGGACACCCGCTCGCGAAGG	23	164	1,072	−	152292	152314
miR-r111.2-4	CCCGAAACTCCGTCGAACGCG	21	418	1,075	−	152762	152782
miR-r111.2-5	TTCCACGTTGTTTCGAGGCCT	21	1,637	3,770	−	152723	152743
miR-r111.2-6	TTCGCGGACGATCGAGGAG	19	14,331	57,461	−	152854	152872
Sequenced from salivary glands (21 dpi)							
miR-r6-1	TCGACCTCAAGCCGTTCGGGAC	22	9	74	+	8671	8692
miR-OriLyt-1	GACGGGGTCTCGGGCTCCTGA	21	22	42	+	77402	77422
miR-OriLyt-2	TGGCTCGCGTCGCCATGGAGACA	23	5	8	+	78953	78975
miR-R87-1	TCGAAGAACGGGTGCAACTC	20	402	926	+	113930	113949
miR-R91-1	GGACTCGGAGTCGTCGGACGCT	22	12	54	+	121165	121186
miR-r111.1-1	CGCACCGGCGTCGAGCACGTAC	22	28	113	+	152214	152235
miR-r111.1-2	TCGAAACAACGTGGAACGGCGT	22	646	1,942	+	152728	152749
miR-r111.1-3	TCGGGGGCGGTCGGAAGGT	19	7	19	+	152891	152909
miR-r170-1	ACCGACTGAGCGGACGG	17	6	6	+	224343	224359
miR-r1-1	GTAAGATGGAATCACCGGAGGC	22	51	198	−	1023	1044
miR-r1-2	TTTCTCTCGTGCTCCGTGTCGC	22	6	6	−	1187	1208
miR-r1-3	TGATGCGGGGTAGGGGAGTGAGA	23	3	3	−	1153	1175
miR-r37-1	TTGTCGTGGGTTTCGT	16	143	147	−	34740	34755
miR-r43.1-1	TTATCAGCCGGCAAGCACCCA	21	15	36	−	40750	40770
miR-r95.1-1	GACGGAGAGCGAACGGT	17	4	4	−	128079	128095
miR-r111.2-2	CTTCGAGTGCGTGTCCGATAG	21	10	20	−	152239	152259
miR-r111.2-3	ATCGGACACCCGCTCGCGAAGGA	23	12	31	−	152291	152313
miR-r111.2-4	CCCGAAACTCCGTCGAACGCG	21	17	30	−	152762	152782
miR-r111.2-5	TTCCACGTTGTTTCGAGGCCT	21	45	101	−	152723	152743
miR-r111.2-6	TTCGCGGACGATCGAGGAGGCC	22	87	399	−	152851	152872

[a] Positions are given relative to the published genomic sequence of the Maastricht strain of RCMV.
[b] Shown is the predominant isoform sequence.

RESULTS

Identification of RCMV miRNAs. To identify the miRNAs encoded by RCMV, we deep sequenced the small RNAs expressed in RCMV-infected fibroblasts and in persistently infected salivary glands from a rat infected for 21 days. We have previously demonstrated that salivary glands from rats infected for 21 days have highly restricted viral gene expression profiles, limited to a small number of genes involved in immune evasion and persistence (65). For sequencing experiments, total RNA was extracted and the small RNAs (15 to 25 bp) were isolated by polyacrylamide gel electrophoresis. The RNAs were ligated to 5′ and 3′ primers and deep sequenced using an Illumina Solexa G1 sequencer. The total reads were filtered for composition, length, and junk.

A total of 6,665,287 reads were made in the RCMV-infected fibroblast sample, and nearly 41% of the sequences were mapped to either the cellular miR database or the rat genome (Table 1). A total of 7,230,718 reads were made in the RCMV-infected salivary gland sample, and nearly 33% of the sequences were mapped to the miR database and/or to the rat genome. Approximately 87% of the sequenced small RNAs from the infected fibroblast sample and 85% from the infected salivary glands were between 19 and 23 bp. A list of the cellular miRNAs detected in the infected fibroblasts and salivary

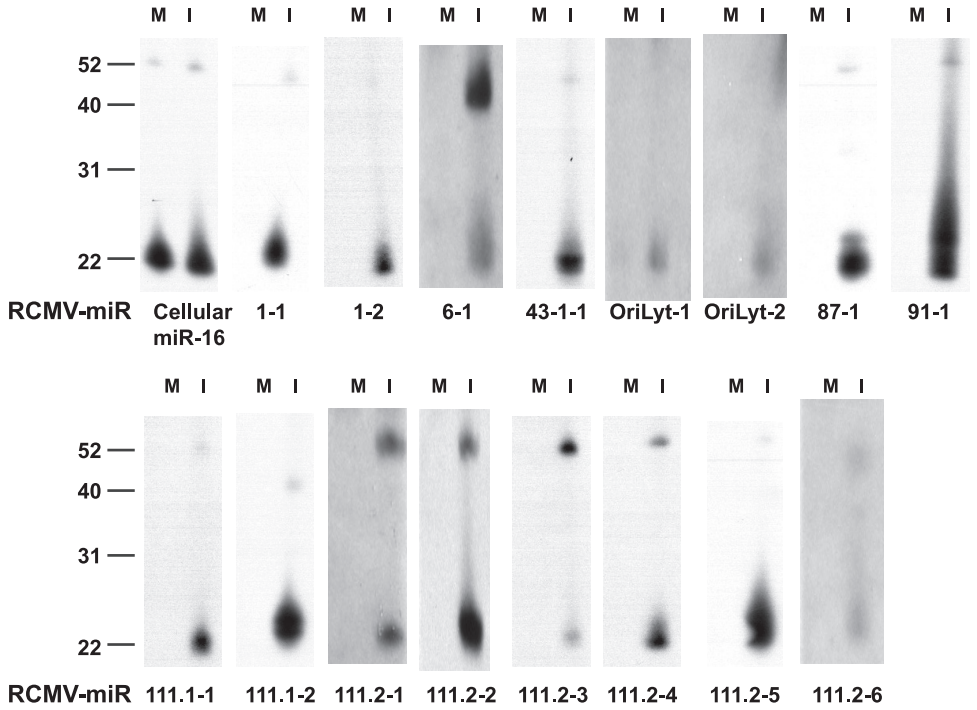

FIG. 1. Northern blot analysis of RCMV miRNAs. RFL6 cells were infected at a multiplicity of 1 PFU per cell and subjected to Northern blot analysis using probes specific for the predicted RCMV miRNA sequences. Lanes M, mock infected; lanes I, infected. The cellular miRNA miR-16 was used as a loading control. The values to the left are molecular sizes in nucleotides.

glands is available at http://www.ohsu.edu/vgti/suppdata.htm. Of the 976,611 unmapped sequences from the RCMV-infected fibroblasts 305,522 (31%) mapped to hairpin structures within the RCMV genome. However, the number of sequences mapping to the RCMV genome from the infected salivary gland sample was only 0.7% of the total reads (4,159 total counts). The remainder of the unmapped sequences most likely represent RNA degradation products, noncoding RNAs, or as-yet-unrealized cellular miRNAs.

We identified 24 unique miRNAs in the RCMV-infected samples (fibroblasts and salivary gland tissue combined) that mapped to hairpin structures found within the viral genome (Table 2; http://www.ohsu.edu/vgti/suppdata.htm). Of the 24 RCMV miRNAs, 22 were expressed in the fibroblast sample, with 4 (miR-r1-4, miR-r43.1-2, miR-R90-1, and miR-r111.2-1) being uniquely detected in this sample and not in salivary gland tissue. Twenty viral miRNAs were detected in the salivary glands; 18 of these were also detected in the fibroblasts, and two RCMV-encoded miRNAs (miR-r95.1-1 and miR-r170-1) were only present in the salivary gland tissues. The viral miRNAs ranged from 16 to 23 nucleotides (nt) in length; however, most were between 19 and 22 nt. As expected, the overall viral miRNA copy number in the salivary glands was lower than in the infected fibroblasts, which is most likely due to the lower infection rate found *in vivo*. Expression profiles (types of miRNAs and relative levels) of the RCMV miRNAs are, for the most part, consistent under both *in vitro* and *in vivo* conditions. Accordingly, the most highly expressed of the viral miRNAs, miR-R87-1, miR-r111.1-2, miR-r111.2-5, and miR-r1-1, are commonly expressed under both conditions (Table 2). A small number of RCMV miRNAs are expressed at low levels, and it is possible that their discovery alone might be due to the high sensitivity of the deep sequencing methods employed for this study. To validate the expression of the RCMV miRNAs, we performed Northern blot analysis of RNA extracted from RCMV-infected RFL6 fibroblasts at 72 hpi. Figure 1 shows the results obtained from 16 out of 24 RCMV miRNAs compared to the control cellular miRNA miR-16. We observed the mature form (~22 nt) of all of the miRNAs, as well as the pre-miRNA forms of some of them.

Identification of RCMV miRNA isoforms. Similar to what has been observed in other studies of viral and cellular miRNAs, a number of the RCMV miRNAs had considerable variation at their 3′ and 5′ ends. As shown in Table 3, the variation, for the most part, was conserved between the miRNAs detected in the infected fibroblasts and those in the rat salivary gland tissues. However, there were specific examples where the percentage of the particular miRNA isoform differed between the two samples. For example, RCMV miR-r6-1 has four major isoforms but only three of these were dominant in the fibroblasts. One of the isoforms of miR-r6-1 (TCGAC CTCAAGCCGTTCGGGGACA) was the most highly expressed isoform detected in salivary gland tissues, but this isoform was expressed to very low levels in fibroblasts. Similarly, one of the isoforms of RCMV miR-OriLyt-2 was only detected in the *in vivo* sample (60% of the sequenced sequences for this miRNA) but not in infected fibroblasts. We also detected the miRNA* (passenger strand) for 13 of the viral miRNAs, and some of these were detected as major isoforms, including those for RCMV miR-r6-1, miR-OriLyt-1, miR-R91-1, and miR-r111.1-1 (Table 3).

TABLE 3. RCMV miRNA sequence isoforms detected in fibroblasts and salivary glands

miR	RCMV miR sequence	Length (nt)	Fibroblasts[a]		Salivary glands[a]	
			Frequency	%	Frequency	%
miR-r6-1	TCGACCTCAAGCCGTTCGGGAC	22	131	13	9	12
	TCCCGTCCACTCCGAGGTCGGT	22	127	13	8	11
	TCGACCTCAAGCCGTTCGGGA	21	97	10	6	8
	TCGACCTCAAGCCGTTCGGGACA	23	25	3	17	23
miR-OriLyt-1	GACGGGGTCTCGGGCTCCTGA	21	178	31	22	52
	GACGGGGTCTCGGGCTCCTGAC	22	110	19	11	26
	CCCGGAGCTCGAAACCCGGTTCG[b]	23	27	5	6	14
miR-OriLyt-2	TGGCTCGCGTCGCCATGGAGAC	22	30	31		ND
	GCTCGCGTCGCCATGGAGACA	21	13	13	3	38
	TGGCTCGCGTCGCCATGGAGACA	23	0	ND	5	62
miR-R87-1	TCGAAGAACGGGTGCAACTC	20	68,629	41	402	43
	TCGAAGAACGGGTGCAACTCT	21	33,774	20	170	18
	GAAGAACGGGTGCAACTC	18	14,028	8	99	11
miR-R91-1	GGACTCGGAGTCGTCGGACGCT	22	1,706	26	12	22
	GGACTCGGAGTCGTCGGACGCTT	23	972	15	12	22
	GACTCGGAGTCGTCGGACGCT	21	467	7	0	ND
	CGTTCGACGATCCCCGGTCCTT[b]	22	191	3	7	13
miR-r111.1-1	CGCACCGGCGTCGAGCACGTAC	22	753	26	28	25
	CGCACCGGCGTCGAGCACGTACT	23	427	15	24	21
	CGCACCGGCGTCGAGCACGT	20	291	10	18	16
	TATGTGCTCGTCACCGGAGGGT[b]	22	333	12	13	12
miR-r111.1-2	TCGAAACAACGTGGAACGGCGT	22	11,212	37	646	33
	TCGAAACAACGTGGAACGGCG	21	4,115	14	161	8
	TCGAAACAACGTGGAACGGCGTT	23	3,707	12	488	25
miR-r1-1	GTAAGATGGAATCACCGGAGG	21	5,265	20	27	14
	GTAAGATGGAATCACCGGAGGC	22	5,234	20	51	26
	GTAAGATGGAATCACCGGAG	20	4,523	17	42	21
	GTAAGATGGAATCACCGGAGGCA	23	3,869	15	34	17
	GTAAGATGGAATCACCGGAGGCT	23	2,748	10	26	13
miR-r1-2	TTTCTCTCGTGCTCCGTGTCGC	22	610	60	6	100
	TTTCTCTCGTGCTCCGTGTCG	21	94	9	0	ND
miR-r43.1-1	TTATCAGCCGGCAAGCACCCAGG	23	1,261	23	9	25
	TTATCAGCCGGCAAGCACCCA	21	1,183	21	15	42
	TTATCAGCCGGCAAGCACCCAG	22	905	16	12	33
miR-r111.2-1	TACGTGCTCGACGCCGGTGCGG	22	13	28	0	ND
	TACGTGCTCGACGCCGGTGCGGA	23	11	23	0	ND
miR-r111.2-2	CTTCGAGTGCGTGTCCGATAGC	22	101	29	5	25
	CTTCGAGTGCGTGTCCGATAG	21	95	27	10	50
	CTTCGAGTGCGTGTCCGATAGT	22	58	17	5	25
miR-r111.2-3	AATCGGACACCCGCTCGCGAAGG	23	164	15	6	20
	AATCGGACACCCGCTCGCGAAG	22	155	14	3	10
	ATCGGACACCCGCTCGCGAAGGA	23	114	11	12	39
	GGACACCCGCTCGCGAAGGA	20	76	7	4	13
miR-r111.2-4	CCCGAAACTCCGTCGAACGCG	21	418	39	17	57
	CCCGAAACTCCGTCGAACGCGC	22	346	32	13	43
miR-r111.2-5	TTCCACGTTGTTTCGAGGCCT	21	1,637	43	45	45
	CACGTTGTTTCGAGGCCT	18	739	20	22	22
miR-r111.2-6	TTCGCGGACGATCGAGGAG	19	14,331	25	77	19
	TTCGCGGACGATCGAGGAGGCC	22	7,799	14	87	22
	TTCGCGGACGATCGAGGAGGC	21	6,162	11	31	8

[a] ND, not detected.
[b] miRNA* or passenger strand sequence.

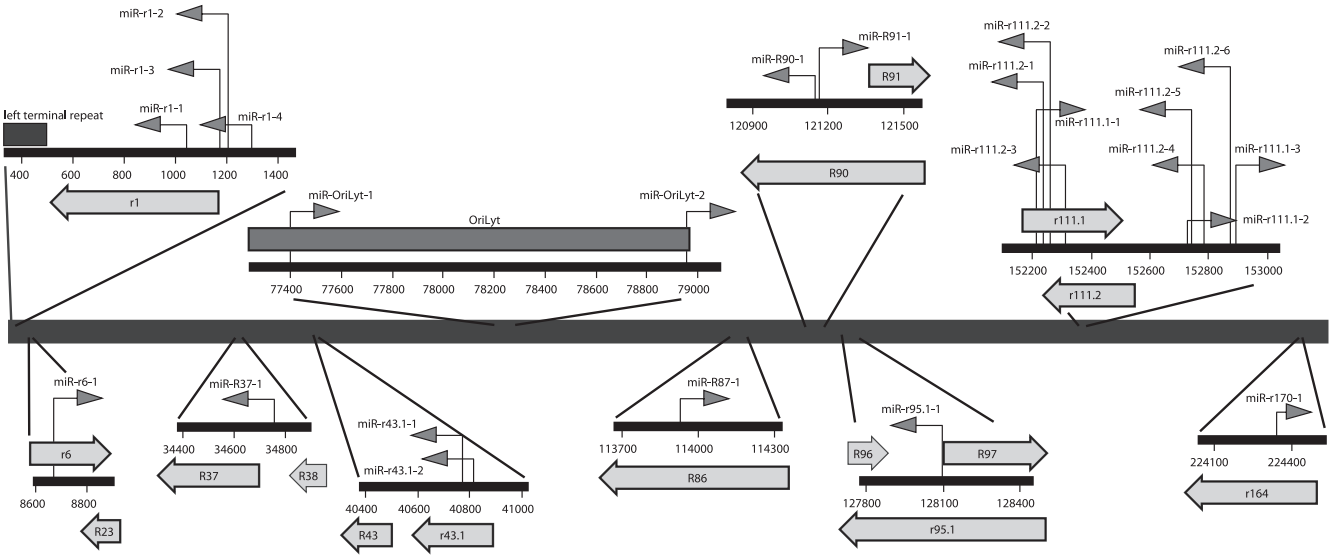

FIG. 2. Genomic organization of RCMV miRNAs. The diagram depicts the regions of the RCMV genome that contain RCMV miRNAs. The dark gray arrows indicate the positions and directions of the RCMV miRNAs, where right-pointing arrows indicate RCMV miRNAs on the sense strand and left-pointing arrows indicate miRNAs on the complement strand. Open reading frames that contain or are near viral miRNAs are shown as light gray block arrows. The RCMV origin of lytic replication is depicted as a dark gray box.

RCMV miRNA genomic organization. The genomic positions of the RCMV miRNAs are depicted in Fig. 2. The RCMV miRNAs are generally distributed across the viral genome. However, similar to what was observed for other herpesviruses, the RCMV miRNAs are often encoded in clusters. The largest cluster of nine viral miRNAs exists in a 700-bp region encoding miR-r111.1-1, miR-r111.1-2, miR-r111.1-3, miR-r111.1-4, miR-r111.2-1, miR-r111.2-2, miR-r111.2-3, miR-r111.2-4, miR-r111.2-5, and miR-r111.2-6. Of these, only two pairs (miR-r111.2-2/miR-r111.2-3 and miR-r111.2-4/miR-r111.2-5) are encoded within the same hairpin loop structure (Fig. 3), indicating that within this region there are at least seven individual hairpin loop structures. A cluster of four viral miRNAs also exists in and near the coding region for the RCMV gene *r1*, and two of these (miR-r1-2/miR-r1-3) also share a hairpin loop. Six of the RCMV-encoded miRNAs could target RCMV mRNAs because they are directly complementary to RCMV genes, including miR-87-1 (R86), miR-R91-1 (R90), and miR-r170-1 (*r164*), as well as miR-r111.2-1, miR-r111.2-2, and miR-r111.2-3, which target r111.1. One additional finding that may have implications for viral persistence is the fact that we identified two viral miRNAs expressed from the viral origin of replication, OriLyt.

We compared the miRNA sequences for mouse cytomegalovirus (MCMV) and RCMV using the phylogenetic analysis program Clustal 3.1. There was minimal conservation between the miRNAs from these two related viruses. However, when we compared the genomic positions of the miRNAs for MCMV and RCMV, we observed that most of them had similar orientations in the viral genomes (Fig. 4). For example, both RCMV and MCMV contain clusters of miRNAs at the extreme 5′ end of the genome. MCMV contains six miRNAs and RCMV contains four miRNAs in this region. RCMV lacks the MCMV genes (*m7* to *m22*), however; RCMV miR-r6-1 is positioned near R23, which is a location similar to that of the cluster of MCMV miRNAs (*m21*, *m22*, and *m23*). Both viral genomes contain miRNAs in or near OriLyt. While the original description of miR-m59-1, -2, and -3 did not suggest this orientation, further review by our group puts these near the origin of lytic replication. Interestingly, both viruses also contain clusters of miRNAs on complementary strands of the viral genomes in a central region near the RCMV and MCMV 112 open reading frames. This region is close to the large stable intron in MCMV and most likely RCMV, although it has not yet been specifically mapped for this virus. It appears that, as in other CMVs, the locations of the RCMV miRNAs share a genome-wide distribution profile, which is different from the observed clustering of the alpha- and gammaherpesvirus miRNAs in latency-associated regions.

Characterization of RCMV miRNA expression. CMV gene expression *in vitro* can be divided into three kinetic classes, immediate early (IE), early, and late, based on the requirements of protein synthesis and viral DNA replication. Therefore, we next sought to determine whether the RCMV miRNAs found within the 700-bp region near RCMV *r111* are all expressed with the same kinetics or differentially regulated. We performed a Northern blot analysis of RNA isolated from RFL6 fibroblasts infected with RCMV for 8, 24, or 48 h, as well as for 48 h in the presence of foscarnet, which differentiates early from late viral gene expression (65). Figure 5 demonstrates that miR-r111.1-1 and miR-r111.2-2 and -3 are expressed with early kinetics as their expression was not inhibited by foscarnet treatment. In contrast, miR-r111.1-2 and -3 and miR-r111.2-1 and -4 were expressed with late kinetics since their expression was blocked at late times in the presence of the viral DNA inhibitor.

Since we found that a portion of the RCMV miRNAs were differentially expressed in fibroblasts and salivary glands, we hypothesized that, similar to viral gene expression in tissues (65), viral miRNA expression is also tissue specific. Therefore,

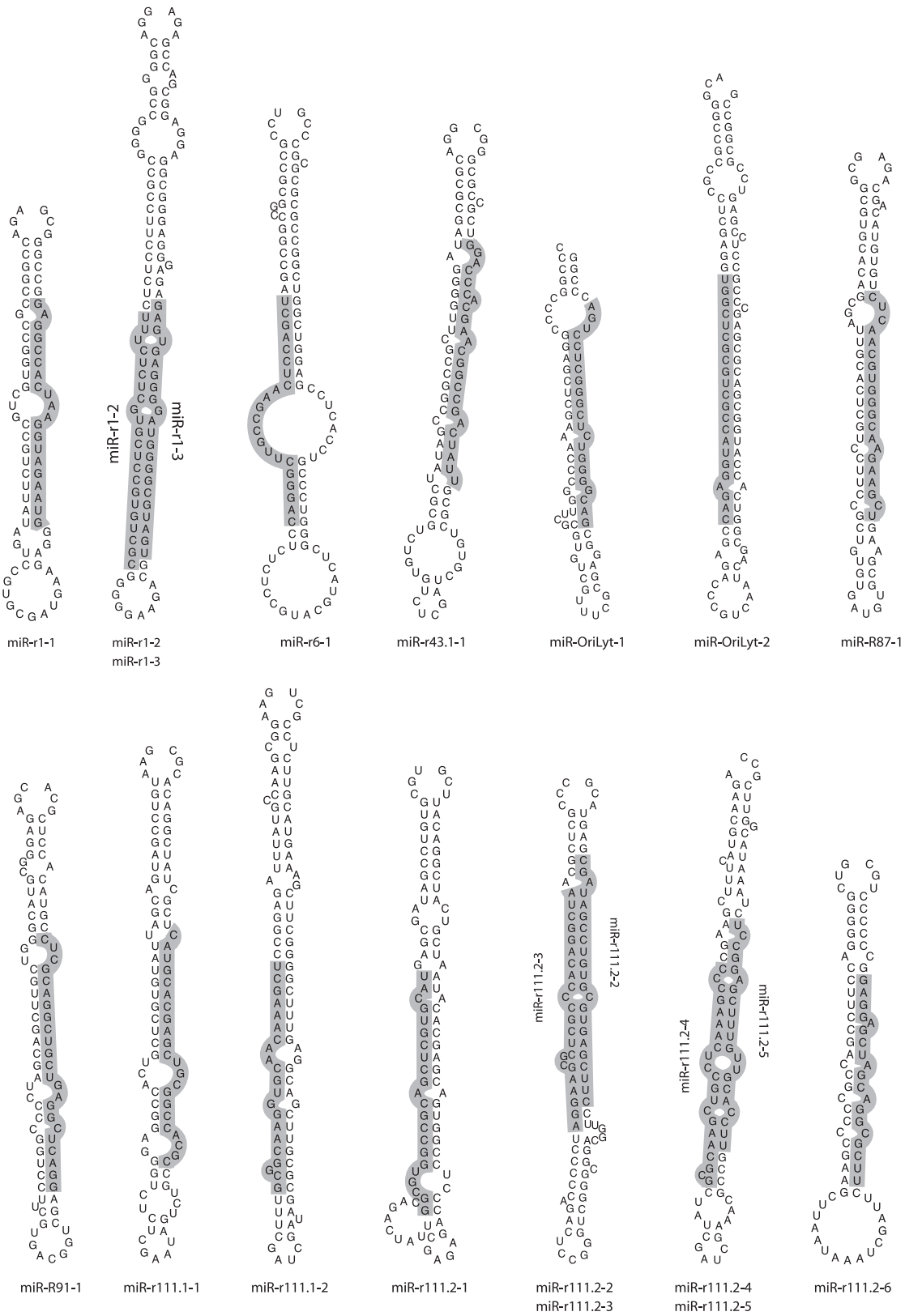

FIG. 3. Secondary structures of RCMV precursor miRNAs. The predicted stem-loop secondary structures of the RCMV pre-miRNAs from the Mfold program (68) are depicted with the mature miRNAs shaded in gray. When two miRNAs are transcribed from one stem-loop, the position of each miRNA is indicated on the 5′ or 3′ arm of the stem-loop.

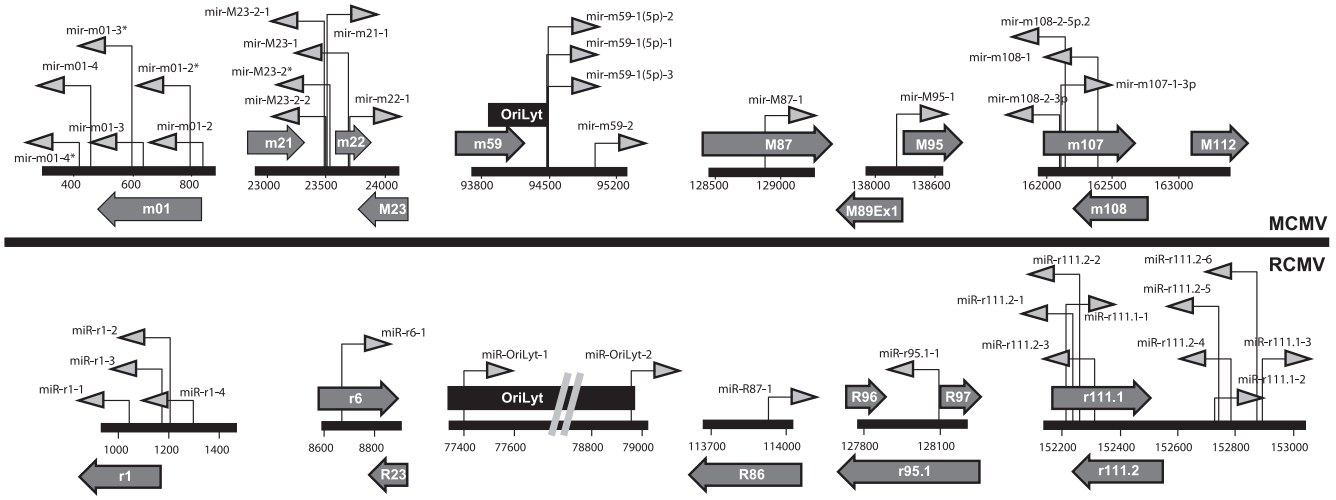

FIG. 4. Comparison of genomic positioning of the RCMV and MCMV miRNAs. The diagram depicts the genomic positioning of the miRNAs expressed by RCMV (lower) and MCMV (upper). The dark gray arrows indicate the positions and directions of the CMV miRNAs, where right-pointing arrows indicate miRNAs on the sense strands and left-pointing arrows indicate miRNAs on the complement strands. Open reading frames that contain or are near viral miRNAs are shown as light gray block arrows. The MCMV and RCMV origins of lytic replication are depicted as black boxes.

we performed real-time PCR analysis of RCMV miR-R87-1 and miR-r111.1-2 with total RNA prepared from the tissues of rat heart allograft recipients harvested at 7 and 28 days posttransplantation. In infected RFL6 fibroblasts, RCMV miR-R87-1 is expressed at higher levels than miR-r111.1-2 (Fig. 6A), which confirmed the sequencing data described above. Similarly, RCMV miR-R87-1 was more highly expressed (by at least 10-fold) than miR-r111.1-2 in tissues from rat heart allograft recipients (Fig. 6B and C). Interestingly, miR-R87-1 was expressed to high levels in all tissues except native heart tissue at 7 days posttransplantation, which is the acute phase of infection. In fact, this viral miRNA was most highly expressed in the allograft heart tissue at day 7. However, miR-R87-1 expression was dramatically reduced to undetectable levels at 28 days in allograft heart, spleen, liver, kidney, and lung tissues. The only tissue that expressed miR-R87-1 at 28 days posttransplantation was the salivary gland, albeit at levels that were 7-fold lower than those measured on day 7. RCMV miR-r111.1-2 is almost exclusively expressed in salivary gland tissues, and the level of expression increased from day 7 to day 28. Importantly, we have previously shown that viral gene expression profiles are tissue specific and the profiles do not correlate with viral DNA loads or viral mRNA levels (65).

DISCUSSION

In the present study, we utilized the robust cloning/sequencing approach (2, 32) to identify the miRNAs expressed by the Maastricht strain of RCMV in cultured fibroblasts, as well as salivary glands from infected rats during the persistent phase of infection. Our study differs from previous studies of CMV miRNA identification in that we sequenced the RCMV miRNAs from both acutely infected cells and *in vivo* persistently infected tissues (7, 15, 16, 21, 47). We identified 24 small RNAs expressed from the RCMV genome that map to regions predicted to fold into stem-loop structures. In fact, many of the RCMV pre-miRNAs were detected by Northern blot analysis. In addition, we cloned and sequenced the corresponding

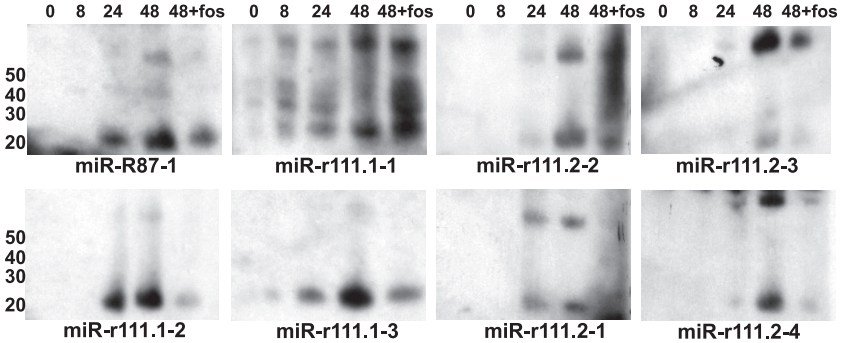

FIG. 5. Kinetic analysis of miRNA expression by Northern blotting. Total RNA was harvested with Trizol from RCMV-infected RFL6 rat fibroblasts at 0, 8, 24, and 48 hpi. Cells were infected at a MOI of 1.0. An additional sample harvested at 48 hpi was treated with Foscavir (foscarnet sodium; 100 mg/ml) to prevent late gene expression. RNA was subjected to Northern blot analysis using probes specific for the predicted RCMV miRNA sequences. Lane 1 (0 hpi) was a mock-infected sample. The values to the left are molecular sizes in nucleotides.

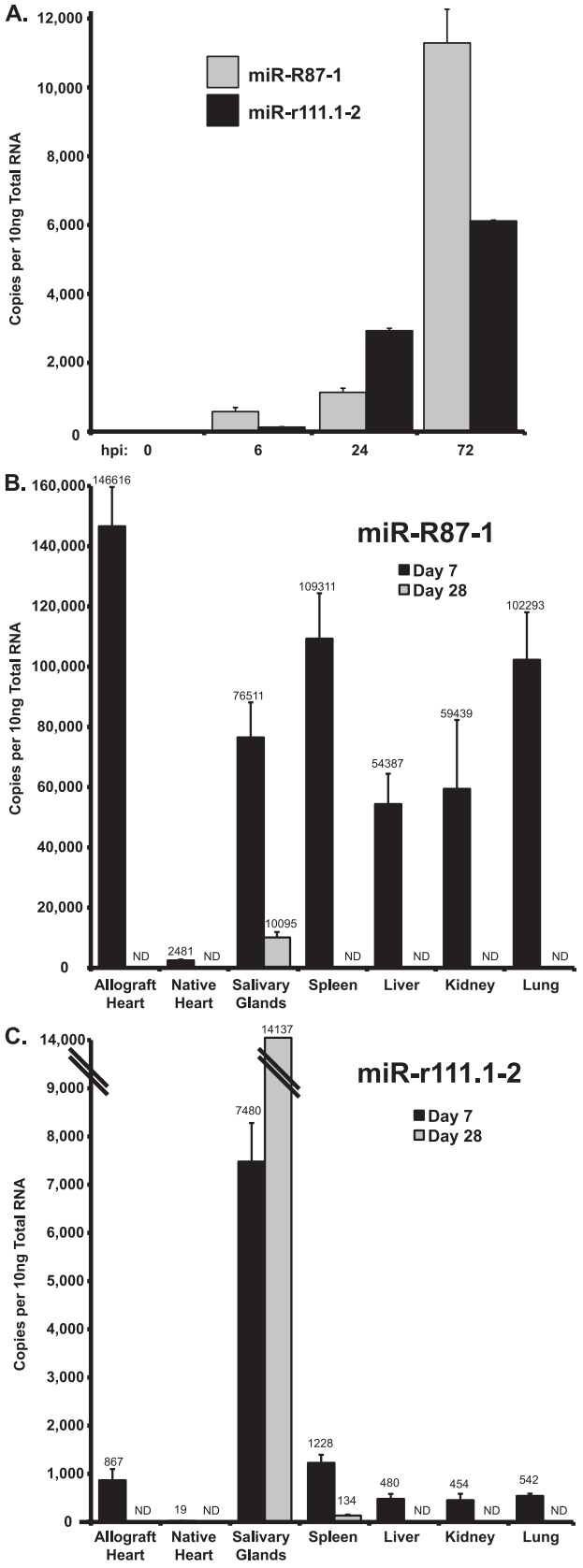

FIG. 6. RCMV miRNA expression in tissues from RCMV-infected allograft recipients. The level of RCMV miRNA expression was determined by RT-PCR analysis of total RNA samples. Shown are viral miRNA copy numbers determined using dilutions of an oligonucleotide standard with the specific miRNA sequences of miR-R87-1 and miR-r111.1-2. (A) Quantification of RCMV miRNA miR-R87-1 and miR-r111.1-2 expression in RCMV-infected fibroblasts at 0, 6, 24, and 72 hpi. Uninfected cells (time zero) were included as a negative control. Both viral miRNAs accumulate with increasing time. (B) RT-PCR results for RCMV miR-R87-1 from tissues harvested from RCMV-infected heart allograft recipients ($n = 3$) at 7 and 28 days posttransplantation. RCMV miR-R87-1 was most highly expressed in the allograft heart, spleen, and lung tissues at 7 days posttransplantation. (C) RT-PCR results for RCMV miR-r111.1-2 from tissues harvested from RCMV-infected heart allograft recipients ($n = 3$). miR-r111.1-2 was most highly expressed in salivary glands at 7 and 28 days posttransplantation. ND, not detected.

miRNA* or passenger strand for a number of the miRNAs discovered in this study. Similar to both HCMV and MCMV miRNAs, the RCMV miRNAs are found distributed individually or in clusters across the viral genome, which differs substantially from their distribution in alpha- and gammaherpesviruses (8, 25, 34, 48, 53, 54). Of the 24 identified RCMV miRNAs, 4 were uniquely detected in the infected fibroblast sample and 2 were unique to the persistently infected salivary gland tissue, which is most likely attributed to the natural variation observed between *in vivo* and *in vitro* infection scenarios (65). The facts that RCMV miR-r111.1-2 was exclusively expressed in salivary glands and its expression increased during persistence whereas miR-R87-1 was downregulated during persistence suggest that viral miRNA expression is dynamic and regulated *in vivo*.

Viral miRNA target discovery and determination of the relevance of this targeting to virus infection have been intrinsically difficult. This problem is compounded for HCMV due to the species specificity of CMVs and the lack of an appropriate *in vivo* animal model for HCMV. However, various *in vitro* and bioinformatic studies have identified both cellular and viral targets of the HCMV miRNAs. For example, miR-UL112 targets the viral transcription factor IE protein IE72 and UL114 targets the virally encoded uracil DNA glycosylase, which is important for the transition to late-phase viral DNA replication (13, 23, 60). A leading hypothesis for the role of miRNAs is in the establishment of latency due to their ability to downregulate IE protein expression especially during the late phase of lytic replication, when the viral miRNAs accumulate to high levels. Subsequently, once latency is established, viral miRNA targeting of the IE genes may help to maintain latency by inhibiting initiation of the lytic cascade. In fact, a common feature of most herpesvirus miRNAs is the targeting of expression of viral transactivators, including the herpes simplex virus type 1 (HSV-1) miR-LAT target ICP0, the Epstein-Barr virus (EBV) miR-BHRF-1 and miR-BART15 targets BZLF1 and BRLF1, respectively, and the Kaposi's sarcoma herpesvirus (KSHV) miR-K10-6-3p targets Rta and Zta (43). In addition, HCMV miR-US25-1 and miR-US25-2 miRNAs may contribute to the establishment of latency since they were recently shown to reduce viral replication and DNA synthesis of not only HCMV but other DNA viruses as well (HSV-1 and adenovirus) (60). Thus, it was hypothesized that miR-US25-1 and miR-US25-2 target cellular genes essential for virus growth. Recently, Grey et al. demonstrated that HCMV miR-US25-1

targets multiple cellular genes related to cell cycle control, specifically, the gene for cyclin E2 (24). Multiple EBV and KSHV miRNAs also target cellular pathways involved in apoptosis and cell cycle regulation (11, 33, 67). HCMV, KSHV, and EBV encode a miRNA that targets the NK cell-activating ligand MICB, and its downregulation leads to decreased viral infected cell killing (59). Thus, it appears that expression of viral miRNAs provides herpesviruses a nonimmunogenic strategy to stably alter the cellular environment during persistence.

Importantly, the types of genes and pathways targeted by viral miRNAs are most likely cell type specific and this fact must be taken into consideration when identifying targets of the viral miRNAs. To date, most of the tissues examined for miRNA expression show that cellular miRNA expression is not only cell type specific but also dependent upon the differentiation of that cell type (3, 34). Examination of miRNA expression in 17 hematopoietic cell lines was compared to that in purified human B cells, T cells, monocytes, and granulocytes and was found to have considerable differences based upon cell type and differentiation status (50). Similarly, differential miRNA expression is documented for viruses. We identified two RCMV miRNAs that were expressed in salivary glands but not in acutely infected fibroblasts and four that were not expressed during persistence in salivary glands (Table 2). In addition, the expression patterns of miR-R87-1 and miR-r111.1-2 differ in their tissue expression and timing following infection (Fig. 6). EBV BART and BHFR miRNAs are controlled by different virus latency programs, and they are differentially expressed in lymphoid and epithelial cells (9, 49). EBV-associated primary tumors have high levels of miR-BART (66). Conversely, in AIDS diffuse large B-cell lymphomas, only BHRF miRNAs were detected but BHRF2 miRNAs were not detected in nasopharyngeal carcinoma tumors (12). An additional level of control of viral miRNA expression and targeting specificity exists due to the heterogeneous processing of the 5′ and 3′ ends of the miRNA. We and others have observed that pre-miRNA processing can produce distinct isoforms of miRNA-miRNA* duplexes with 5′ and 3′ heterogeneity (Table 3 and reference 10). The mechanisms of how miRNA isoforms are derived and the extent of their differential function are still unknown. However, recent studies provide evidence to suggest that miRNA length isoforms are relatively common and that a single pre-miRNA hairpin can be differentially processed to give rise to several functional miRNAs with various biological properties (1, 17–19). Interestingly, the differences in biological function may be attributed to the fact that the length isoforms can utilize unique Argonaute-RISC protein complexes (17). Alternative processing at the 5′ end would switch the seed sequence of the miRNA, alter target recognition, and act to broaden the regulatory impact of the miRNA (19). Interestingly, we also observed differential isoform usage between the *in vitro* fibroblast samples and the *in vivo* salivary gland samples. A specific isoform of miR-OriLyt-2 was only detected in the salivary gland sample and not in the fibroblast sample. This finding highlights the importance of determining the role of miRNA heterogeneity *in vivo*. Thus, herpesvirus miRNAs possibly play particular roles during the infection of differentiated cell types, making it critical to understand cell and tissue type-specific miRNA expression in order to elucidate miRNA function.

An important characteristic of the miRNAs encoded by MCMV and RCMV is the finding that there are at least two miRNAs for each virus encoded in or directly adjacent to the origin of lytic replication. The function of these miRNAs is still unknown. However, they may play an important role in viral DNA replication. It has been shown that a small RNA stem-loop structure encoded by EBV mediates the recruitment of the origin recognition complex to OriP by binding ORC1 and the RGG motifs of EBNA-1 (44). This promotes the assembly of the replication complex at OriP but occurs in the absence of RNA-DNA binding. Thus, another plausible role for viral miRNAs encoded in OriLyt might be in DNA replication by directly binding DNA at the origin. It is possible that the viral miRNA might act as the RNA primer, normally synthesized by the host primase, that base pairs with the DNA at the origin of replication to initiate DNA synthesis. This would be especially important for the initiation of viral DNA synthesis in nondividing cells during reactivation from latency. Further experimentation to characterize the role of these miRNAs in viral replication is warranted and may lead to the development of novel therapeutics that target and exploit this interesting relationship. The aim of this study was to identify the small RNAs encoded in the RCMV genome and determine *in vivo* viral miRNA expression in RCMV-infected rats. This knowledge will enable us to characterize the *in vivo* roles and relevance of CMV-encoded miRNAs during acute and persistent infections, latency/reactivation, and pathogenesis.

ACKNOWLEDGMENTS

This work was supported by research grants from the National Institutes of Health to D. N. Streblow (HL083194) and S. L. Orloff (HL085451).

REFERENCES

1. **Ameres, S. L., M. D. Horwich, J. H. Hung, J. Xu, M. Ghildiyal, Z. Weng, and P. D. Zamore.** 2010. Target RNA-directed trimming and tailing of small silencing RNAs. Science **328:**1534–1539.
2. **Babiarz, J. E., J. G. Ruby, Y. Wang, D. P. Bartel, and R. Blelloch.** 2008. Mouse ES cells express endogenous shRNAs, siRNAs, and other Microprocessor-independent, Dicer-dependent small RNAs. Genes Dev. **22:**2773–2785.
3. **Bartel, D. P.** 2004. MicroRNAs: genomics, biogenesis, mechanism, and function. Cell **116:**281–297.
4. **Bartel, D. P., and C. Z. Chen.** 2004. Micromanagers of gene expression: the potentially widespread influence of metazoan microRNAs. Nat. Rev. Genet. **5:**396–400.
5. **Beisser, P. S., C. Vink, J. G. Van Dam, G. Grauls, S. J. Vanherle, and C. A. Bruggeman.** 1998. The R33 G protein-coupled receptor gene of rat cytomegalovirus plays an essential role in the pathogenesis of viral infection. J. Virol. **72:**2352–2363.
6. **Bruggeman, C. A., H. Schellekens, G. Grauls, W. M. Debie, and C. P. van Boven.** 1983. Rat cytomegalovirus: induction of and sensitivity to interferon. Antiviral Res. **3:**315–324.
7. **Buck, A. H., J. Santoyo-Lopez, K. A. Robertson, D. S. Kumar, M. Reczko, and P. Ghazal.** 2007. Discrete clusters of virus-encoded microRNAs are associated with complementary strands of the genome and the 7.2-kilobase stable intron in murine cytomegalovirus. J. Virol. **81:**13761–13770.
8. **Cai, X., and B. R. Cullen.** 2006. Transcriptional origin of Kaposi's sarcoma-associated herpesvirus microRNAs. J. Virol. **80:**2234–2242.
9. **Cai, X., A. Schäfer, S. Lu, J. P. Bilello, R. C. Desrosiers, R. Edwards, N. Raab-Traub, and B. R. Cullen.** 2006. Epstein-Barr virus microRNAs are evolutionarily conserved and differentially expressed. PLoS Pathog. **2:**e23.
10. **Chiang, H. R., L. W. Schoenfeld, J. G. Ruby, V. C. Auyeung, N. Spies, D. Baek, W. K. Johnston, C. Russ, S. Luo, J. E. Babiarz, R. Blelloch, G. P. Schroth, C. Nusbaum, and D. P. Bartel.** 2010. Mammalian microRNAs: experimental evaluation of novel and previously annotated genes. Genes Dev. **24:**992–1009.
11. **Choy, E. Y., K. L. Siu, K. H. Kok, R. W. Lung, C. M. Tsang, K. F. To, D. L. Kwong, S. W. Tsao, and D. Y. Jin.** 2008. An Epstein-Barr virus-encoded microRNA targets PUMA to promote host cell survival. J. Exp. Med. **205:** 2551–2560.

12. **Cosmopoulos, K., M. Pegtel, J. Hawkins, H. Moffett, C. Novina, J. Middeldorp, and D. A. Thorley-Lawson.** 2009. Comprehensive profiling of Epstein-Barr virus microRNAs in nasopharyngeal carcinoma. J. Virol. **83:**2357–2367.
13. **Courcelle, C. T., J. Courcelle, M. N. Prichard, and E. S. Mocarski.** 2001. Requirement for uracil-DNA glycosylase during the transition to late-phase cytomegalovirus DNA replication. J. Virol. **75:**7592–7601.
14. **de Otero, J., J. Gavalda, E. Murio, et al.** 1998. Cytomegalovirus disease as a risk factor for graft loss and death after orthotopic liver transplantation. Clin. Infect. Dis. **26:**865–870.
15. **Dölken, L., J. Perot, V. Cognat, A. Alioua, M. John, J. Soutschek, Z. Ruzsics, U. Koszinowski, O. Voinnet, and S. Pfeffer.** 2007. Mouse cytomegalovirus microRNAs dominate the cellular small RNA profile during lytic infection and show features of posttranscriptional regulation. J. Virol. **81:**13771–13782.
16. **Dunn, W., P. Trang, Q. Zhong, E. Yang, C. van Belle, and F. Liu.** 2005. Human cytomegalovirus expresses novel microRNAs during productive viral infection. Cell. Microbiol. **7:**1684–1695.
17. **Ebhardt, H. A., A. Fedynak, and R. P. Fahlman.** 2010. Naturally occurring variations in sequence length creates microRNA isoforms that differ in Argonaute effector complex specificity. Silence **1:**12.
18. **Ebhardt, H. A., H. H. Tsang, D. C. Dai, Y. Liu, B. Bostan, and R. P. Fahlman.** 2009. Meta-analysis of small RNA-sequencing errors reveals ubiquitous post-transcriptional RNA modifications. Nucleic Acids Res. **37:**2461–2470.
19. **Ghildiyal, M., J. Xu, H. Seitz, Z. Weng, and P. D. Zamore.** 2010. Sorting of Drosophila small silencing RNAs partitions microRNA* strands into the RNA interference pathway. RNA **16:**43–56.
20. **Grattan, M. T., C. E. Moreno-Cabral, V. A. Starnes, P. E. Oyer, E. B. Stinson, and N. E. Shumway.** 1989. Cytomegalovirus infection is associated with cardiac allograft rejection and atherosclerosis. JAMA **261:**3561–3566.
21. **Grey, F., A. Antoniewicz, E. Allen, J. Saugstad, A. McShea, J. C. Carrington, and J. Nelson.** 2005. Identification and characterization of human cytomegalovirus-encoded microRNAs. J. Virol. **79:**12095–12099.
22. **Grey, F., L. Hook, and J. Nelson.** 2008. The functions of herpesvirus-encoded microRNAs. Med. Microbiol. Immunol. **197:**261–267.
23. **Grey, F., H. Meyers, E. A. White, D. H. Spector, and J. Nelson.** 2007. A human cytomegalovirus-encoded microRNA regulates expression of multiple viral genes involved in replication. PLoS Pathog. **3:**e163.
24. **Grey, F., R. Tirabassi, H. Meyers, G. Wu, S. McWeeney, L. Hook, and J. A. Nelson.** 2010. A viral microRNA down-regulates multiple cell cycle genes through mRNA 5′UTRs. PLoS Pathog. **6:**e1000967.
25. **Grundhoff, A., C. S. Sullivan, and D. Ganem.** 2006. A combined computational and microarray-based approach identifies novel microRNAs encoded by human gamma-herpesviruses. RNA **12:**733–750.
26. **Handa, N., M. Hatanaka, W. A. Baumgartner, B. A. Reitz, G. Sandford, A. H. Esa, and A. Herskowitz.** 1993. Late cyclosporine treatment ameliorates established coronary graft disease in rat allografts. Transplantation **56:**535–540.
27. **Hillebrands, J. L., J. G. van Dam, G. Onuta, F. A. Klatter, G. Grauls, C. A. Bruggeman, and J. Rozing.** 2005. Cytomegalovirus-enhanced development of transplant arteriosclerosis in the rat; effect of timing of infection and recipient responsiveness. Transpl. Int. **18:**735–742.
28. **Kloover, J. S., J. L. Hillebrands, G. de Wit, G. Grauls, J. Rozing, C. A. Bruggeman, and P. Nieuwenhuis.** 2000. Rat cytomegalovirus replication in the salivary glands is exclusively confined to striated duct cells. Virchows Arch. **437:**413–421.
29. **Kloppenburg, G., R. de Graaf, S. Herngreen, G. Grauls, C. Bruggeman, and F. Stassen.** 2005. Cytomegalovirus aggravates intimal hyperplasia in rats by stimulating smooth muscle cell proliferation. Microbes Infect. **7:**164–170.
30. **Koskinen, P., K. Lemström, S. Mattila, P. Hayry, and M. S. Nieminen.** 1996. Cytomegalovirus infection associated accelerated heart allograft arteriosclerosis may impair the late function of the graft. Clin. Transplant. **10:**487–493.
31. **Koskinen, P. K., S. Yilmaz, E. Kallio, C. A. Bruggeman, P. J. Hayry, and K. Lemström.** 1996. Rat cytomegalovirus infection and chronic kidney allograft rejection. Transpl. Int. **9:**S3–S4.
32. **Kuchenbauer, F., R. D. Morin, B. Argiropoulos, O. I. Petriv, M. Griffith, M. Heuser, E. Yung, J. Piper, A. Delaney, A. L. Prabhu, Y. Zhao, H. McDonald, T. Zeng, M. Hirst, C. L. Hansen, M. A. Marra, and R. K. Humphries.** 2008. In-depth characterization of the microRNA transcriptome in a leukemia progression model. Genome Res. **18:**1787–1797.
33. **Lagana, A., S. Forte, F. Russo, R. Giugno, A. Pulvirenti, and A. Ferro.** 2010. Prediction of human targets for viral-encoded microRNAs by thermodynamics and empirical constraints. J. RNAi Gene Silencing **6:**379–385.
34. **Landgraf, P., M. Rusu, R. Sheridan, A. Sewer, N. Iovino, A. Aravin, S. Pfeffer, A. Rice, A. O. Kamphorst, M. Landthaler, C. Lin, N. D. Socci, L. Hermida, V. Fulci, S. Chiaretti, R. Foa, J. Schliwka, U. Fuchs, A. Novosel, R. U. Muller, B. Schermer, U. Bissels, J. Inman, Q. Phan, M. Chien, D. B. Weir, R. Choksi, G. De Vita, D. Frezzetti, H. I. Trompeter, V. Hornung, G. Teng, G. Hartmann, M. Palkovits, R. Di Lauro, P. Wernet, G. Macino, C. E. Rogler, J. W. Nagle, J. Ju, F. N. Papavasiliou, T. Benzing, P. Lichter, W. Tam, M. J. Brownstein, A. Bosio, A. Borkhardt, J. J. Russo, C. Sander, M. Zavolan, and T. Tuschl.** 2007. A mammalian microRNA expression atlas based on small RNA library sequencing. Cell **129:**1401–1414.
35. **Lee, R. C., R. L. Feinbaum, and V. Ambros.** 1993. The C. elegans heterochronic gene lin-4 encodes small RNAs with antisense complementarity to lin-14. Cell **75:**843–854.
36. **Lemström, K. B., P. T. Aho, C. A. Bruggeman, and P. J. Hayry.** 1994. Cytomegalovirus infection enhances mRNA expression of platelet-derived growth factor-BB and transforming growth factor-beta I in rat aortic allografts. Possible mechanism for cytomegalovirus-enhanced graft arteriosclerosis. Arterioscler. Thromb. **14:**2043–2052.
37. **Lemström, K. B., J. H. Bruning, C. A. Bruggeman, P. Koskinen, P. T. Aho, S. Yilmaz, I. T. Lautenschlager, and P. J. Hayry.** 1994. Cytomegalovirus infection-enhanced allograft arteriosclerosis is prevented by DHPG prophylaxis in the rat. Circulation **90:**1969–1978.
38. **Lemström, K. B., P. K. Koskinen, J. H. Bruning, C. A. Bruggeman, I. T. Lautenschlager, and P. J. Hayry.** 1994. Effect of ganciclovir prophylaxis on cytomegalovirus-enhanced allograft arteriosclerosis. Transpl. Int. **7**(Suppl. 1)**:**S383–S384.
39. **Martelius, T., M. Scholz, L. Krogerus, K. Hockerstedt, R. Loginov, C. Bruggeman, J. Cinatl, Jr., H. W. Doerr, and I. Lautenschlager.** 1999. Antiviral and immunomodulatory effects of desferrioxamine in cytomegalovirus-infected rat liver allografts with rejection. Transplantation **68:**1753–1761.
40. **Melnick, J. L., E. Adam, and M. E. DeBakey.** 1998. The link between CMV and atherosclerosis. Infect. Med. **15:**479–486.
41. **Melnick, J. L., B. L. Petrie, G. R. Dreesman, J. Burek, C. H. McCollum, and M. E. DeBakey.** 1983. Cytomegalovirus antigen within human arterial smooth muscle cells. Lancet **2**(8351)**:**644–647.
42. **Melnychuk, R. M., D. N. Streblow, P. P. Smith, A. J. Hirsch, D. Pancheva, and J. A. Nelson.** 2004. Human cytomegalovirus-encoded G protein-coupled receptor US28 mediates smooth muscle cell migration through Galpha12. J. Virol. **78:**8382–8391.
43. **Murphy, E., J. Vanicek, H. Robins, T. Shenk, and A. J. Levine.** 2008. Suppression of immediate-early viral gene expression by herpesvirus-coded microRNAs: implications for latency. Proc. Natl. Acad. Sci. U. S. A. **105:**5453–5458.
44. **Norseen, J., A. Thomae, V. Sridharan, A. Aiyar, A. Schepers, and P. M. Lieberman.** 2008. RNA-dependent recruitment of the origin recognition complex. EMBO J. **27:**3024–3035.
45. **Orloff, S. L., D. N. Streblow, C. Soderberg-Naucler, Q. Yin, C. Kreklywich, C. L. Corless, P. A. Smith, C. B. Loomis, L. K. Mills, J. W. Cook, C. A. Bruggeman, J. A. Nelson, and C. R. Wagner.** 2002. Elimination of donor-specific alloreactivity prevents cytomegalovirus-accelerated chronic rejection in rat small bowel and heart transplants. Transplantation **73:**679–688.
46. **Persoons, M. C. J., M. J. A. P. Daemen, E. M. van Kleef, G. E. L. M. Grauls, E. Wijers, and C. A. Bruggeman.** 1997. Neointimal smooth muscle cell phenotype is important in its susceptibility to cytomegalovirus (CMV) infection: a study in rat. Cardiovasc. Res. **36:**282–288.
47. **Pfeffer, S., A. Sewer, M. Lagos-Quintana, R. Sheridan, C. Sander, F. A. Grasser, L. F. van Dyk, C. K. Ho, S. Shuman, M. Chien, J. J. Russo, J. Ju, G. Randall, B. D. Lindenbach, C. M. Rice, V. Simon, D. D. Ho, M. Zavolan, and T. Tuschl.** 2005. Identification of microRNAs of the herpesvirus family. Nat. Methods **2:**269–276.
48. **Pfeffer, S., M. Zavolan, F. A. Grasser, M. Chien, J. J. Russo, J. Ju, B. John, A. J. Enright, D. Marks, C. Sander, and T. Tuschl.** 2004. Identification of virus-encoded microRNAs. Science **304:**734–736.
49. **Pratt, Z. L., M. Kuzembayeva, S. Sengupta, and B. Sugden.** 2009. The microRNAs of Epstein-Barr virus are expressed at dramatically differing levels among cell lines. Virology **386:**387–397.
50. **Ramkissoon, S. H., L. A. Mainwaring, Y. Ogasawara, K. Keyvanfar, J. P. McCoy, Jr., E. M. Sloand, S. Kajigaya, and N. S. Young.** 2006. Hematopoietic-specific microRNA expression in human cells. Leuk. Res. **30:**643–647.
51. **Rana, T. M.** 2007. Illuminating the silence: understanding the structure and function of small RNAs. Nat. Rev. Mol. Cell Biol. **8:**23–36.
52. **Rubin, R. H.** 1999. Importance of CMV in the transplant population. Transpl. Infect. Dis. **1**(Suppl. 1)**:**3–7.
53. **Samols, M. A., J. Hu, R. L. Skalsky, and R. Renne.** 2005. Cloning and identification of a microRNA cluster within the latency-associated region of Kaposi's sarcoma-associated herpesvirus. J. Virol. **79:**9301–9305.
54. **Schäfer, A., X. Cai, J. P. Bilello, R. C. Desrosiers, and B. R. Cullen.** 2007. Cloning and analysis of microRNAs encoded by the primate gamma-herpesvirus rhesus monkey rhadinovirus. Virology **364:**21–27.
55. **Skalsky, R. L., and B. R. Cullen.** 2010. Viruses, microRNAs, and host interactions. Annu. Rev. Microbiol. **64:**123–141.
56. **Soule, J. L., D. N. Streblow, T. F. Andoh, C. N. Kreklywich, and S. L. Orloff.** 2006. Cytomegalovirus accelerates chronic allograft nephropathy in a rat renal transplant model with associated provocative chemokine profiles. Transplant. Proc. **38:**3214–3220.
57. **Speir, E., R. Modali, E. S. Huang, M. B. Leon, F. Shawl, T. Finkel, and S. E. Epstein.** 1994. Potential role of human cytomegalovirus and p53 interaction in coronary restenosis. Science **265:**391–394.
58. **Steinhoff, G., X. M. You, C. Steinmuller, K. Boeke, F. S. Stals, C. A. Bruggeman, and A. Haverich.** 1995. Induction of endothelial adhesion molecules by rat cytomegalovirus in allogeneic lung transplantation in the rat. Scand. J. Infect. Dis. Suppl. **99:**58–60.

59. **Stern-Ginossar, N., N. Elefant, A. Zimmermann, D. G. Wolf, N. Saleh, M. Biton, E. Horwitz, Z. Prokocimer, M. Prichard, G. Hahn, D. Goldman-Wohl, C. Greenfield, S. Yagel, H. Hengel, Y. Altuvia, H. Margalit, and O. Mandelboim.** 2007. Host immune system gene targeting by a viral miRNA. Science **317:**376–381.
60. **Stern-Ginossar, N., N. Saleh, M. D. Goldberg, M. Prichard, D. G. Wolf, and O. Mandelboim.** 2009. Analysis of human cytomegalovirus-encoded microRNA activity during infection. J. Virol. **83:**10684–10693.
61. **Streblow, D. N., J. Dumortier, A. V. Moses, S. L. Orloff, and J. A. Nelson.** 2008. Mechanisms of cytomegalovirus-accelerated vascular disease: induction of paracrine factors that promote angiogenesis and wound healing. Curr. Top. Microbiol. Immunol. **325:**397–415.
62. **Streblow, D. N., C. Kreklywich, Q. Yin, V. T. De La Melena, C. L. Corless, P. A. Smith, C. Brakebill, J. W. Cook, C. Vink, C. A. Bruggeman, J. A. Nelson, and S. L. Orloff.** 2003. Cytomegalovirus-mediated upregulation of chemokine expression correlates with the acceleration of chronic rejection in rat heart transplants. J. Virol. **77:**2182–2194.
63. **Streblow, D. N., C. N. Kreklywich, T. Andoh, A. V. Moses, J. Dumortier, P. P. Smith, V. Defilippis, K. Fruh, J. A. Nelson, and S. L. Orloff.** 2008. The role of angiogenic and wound repair factors during CMV-accelerated transplant vascular sclerosis in rat cardiac transplants. Am. J. Transplant. **8:**277–287.
64. **Streblow, D. N., C. N. Kreklywich, P. Smith, J. L. Soule, C. Meyer, M. Yin, P. Beisser, C. Vink, J. A. Nelson, and S. L. Orloff.** 2005. Rat cytomegalovirus-accelerated transplant vascular sclerosis is reduced with mutation of the chemokine-receptor R33. Am. J. Transplant. **5:**436–442.
65. **Streblow, D. N., K. W. van Cleef, C. N. Kreklywich, C. Meyer, P. Smith, V. Defilippis, F. Grey, K. Fruh, R. Searles, C. Bruggeman, C. Vink, J. A. Nelson, and S. L. Orloff.** 2007. Rat cytomegalovirus gene expression in cardiac allograft recipients is tissue specific and does not parallel the profiles detected in vitro. J. Virol. **81:**3816–3826.
66. **Xia, T., A. O'Hara, I. Araujo, J. Barreto, E. Carvalho, J. B. Sapucaia, J. C. Ramos, E. Luz, C. Pedroso, M. Manrique, N. L. Toomey, C. Brites, D. P. Dittmer, and W. J. Harrington, Jr.** 2008. EBV microRNAs in primary lymphomas and targeting of CXCL-11 by ebv-mir-BHRF1-3. Cancer Res. **68:**1436–1442.
67. **Ziegelbauer, J. M., C. S. Sullivan, and D. Ganem.** 2009. Tandem array-based expression screens identify host mRNA targets of virus-encoded microRNAs. Nat. Genet. **41:**130–134.
68. **Zuker, M.** 2003. Mfold web server for nucleic acid folding and hybridization prediction. Nucleic Acids Res. **31:**3406–3415.